Volume 24, No 1 | International Journal of Radiation Research, January 2026

The diagnostic performance of differentiating cervical metastatic lymphadenopathy and tuberculous nodes by shear wave elastography and contrast-enhanced ultrasonography

F. Jia, S. Feng, T. Song, X. Wang*

Department of Ultrasound, The First Affiliated Hospital of Xinjiang Medical University, Urumchi, Xinjiang, China

► ***Original article***

Corresponding author:
Xiaorong Wang, M.D.
E-mail: *pznjiafang@163.com*

Received: March 2025
Final revised: May 2025
Accepted: June 2025

Int. J. Radiat. Res., January 2026; 24(1): 49-54

DOI: 10.61186/ijrr.24.1.8

Keywords: *CEUS and SWE complement each other in differentiating metastatic lymphadenopathy from tuberculous nodes.*

ABSTRACT

Background: To investigate the diagnostic efficacy of shear wave elastography (SWE) and contrast-enhanced ultrasonography (CEUS) in differentiating between metastatic and tuberculous cervical lymphadenopathy. ***Materials and Methods:*** This study included 84 patients with 91 cervical lymph nodes (LNs) that exhibited suspicious malignant features on ultrasonography (US). SWE and CEUS were sequentially performed, followed by analysis of two-dimensional SWE (2D-SWE) characteristics, maximum shear wave elastic modulus (Max-SWE), and CEUS parameters. Cervical lymphadenopathy was categorized as metastatic or tuberculous based on histopathological diagnosis. Diagnostic performance parameters including sensitivity (Se), specificity (Sp), accuracy (Acc), and area under the receiver operating characteristic curve (AUC) of conventional US, SWE, and CEUS were compared. ***Results:*** Conventional US findings showed no significant differences between the groups ($P > 0.05$), whereas 2D-SWE, Max-SWE, and CEUS demonstrated significant differences (all $P < 0.05$). CEUS, 2D-SWE, and Max-SWE demonstrated AUC values of 0.762, 0.643, and 0.605, respectively. 2D-SWE exhibited the highest specificity (Sp, 71.4%), whereas CEUS achieved superior sensitivity (Se, 81.6%) and accuracy (Acc, 75.8%). ***Conclusion:*** CEUS and SWE complement each other in differentiating metastatic lymphadenopathy from tuberculous nodes.

INTRODUCTION

The differential diagnosis of cervical lymphadenopathy is a major challenge in clinical practice, especially the differentiation between metastatic lymphadenopathy and tuberculous lymphadenitis (tuberculous nodules), which often leads to misdiagnosis or delayed treatment due to their similar imaging manifestations [1]. At present, although traditional ultrasound is widely used for LNs evaluation, it mainly relies on morphological parameters (e.g., length-to-diameter ratio, portal structure) and blood flow signal characteristics, with low sensitivity and specificity [2], which is difficult to meet the demand for accurate diagnosis and treatment. Especially in areas with a high incidence of tuberculosis, there is a high overlap between the images of the two lesions, and there is an urgent need to develop new noninvasive techniques to break through the diagnostic bottleneck [3].

In recent years, the combined application of shear wave elastography (SWE) and contrast-enhanced ultrasound (CEUS) has provided a new perspective for the identification of LNs lesions [4]. SWE can reveal microstructural differences in lesions by quantifying tissue stiffness (elastic modulus) - metastatic LNs are usually stiffer due to cancer cell infiltration and fibrosis, whereas tuberculous nodes show a heterogeneous elastic distribution due to caseous necrosis and inflammatory exudates [5]. By dynamically observing the microvascular perfusion pattern, CEUS can distinguish the disordered neovascularization of metastases from the delayed enhancement features of tuberculous granulomas [6].

However, studies on the application of SWE and CEUS in the evaluation of metastatic lymphadenopathy and tuberculous lymphadenitis are rare. This study is the first to integrate the quantitative parameters of SWE elasticity and CEUS time-intensity curve (TIC) characteristics to analyze the effect of both on the assessment of LNs lesions, and these results will provide high-level evidence-based evidence for the noninvasive diagnosis of LNs lesions, which is of great practical significance for optimizing clinical decision-making, reducing medical costs, and improving the prognosis of patients.

MATERIALS AND METHODS

Research object

Patients with cervical lymph node (LNs) enlargement who were admitted to our hospital for treatment between January 2018 and April 2020 were collected. Inclusion criteria for this study: (1). The patient had not received any diagnostic or therapeutic intervention prior to the ultrasound examination; (2) Cervical lymphadenopathy was

[DOI: 10.61186/ijrr.24.1.8]

defined as a short-axis diameter ≥0.8 cm in levels Ib (submandibular) and II (upper jugular), and ≥0.5 cm in levels Ia (submental), III (mid-jugular), IV (lower jugular), and V (posterior triangle); (3) Conventional ultrasound examinations revealed at least 3 suspicious features indicative of malignancy, including (i) a luminal to solid ratio <2, (ii) eccentricity or disappearance of the hilar medulla, (iii) non-uniform echo patterns, and (iv) non-central hilar blood flow abnormalities. Conventional assessment integrating medical history and physical examination failed to reliably differentiate benign from malignant LNs (LNs), particularly those with a depth ≤3 cm from the skin surface [7]; (4) Patients who are ineligible for ultrasound due to contraindications related to non-sonographic contrast agents, such as SonoVue, were excluded from the study; (5) Fine needle aspiration (FNA) or surgical biopsy were conducted to establish definitive histopathological diagnoses. Excluded criteria: (1) Long diameter > 3cm LNs; (2) LNs are located at cervical level VI (paratracheal in the anterior cervical region) or level VII (upper mediastinal tracheoesophageal groove); (3) Pathologically non-tuberculous and non-metastatic LNs. The informed consent was signed after informing the patients of the possible risks. Image acquisition in all cases was undertaken by a senior physician. In conclusion, 91 LNs (LNs) were included in 84 patients, among 40 males and 44 females, aged between 18 and 81 years, with an average age of 44.3±16.4 years. The study was approved by the Ethics Committee of The First Affiliated Hospital of Xinjiang Medical University (No. K202105-10).

Instruments and methods

Conventional ultrasonography was conducted using an SL15-4 MHz transducer (Supersonic Aixplorer ultrasound system, Supersonic Imagine, France). Record (1) L/S: ≥2, <2; (2) Lymphatic hilum medulla morphology: eccentric, disappeared; (3) Internal echo: uniform hypoechoic, non-uniform echo including ballistically slightly hyper-echoic regions, small strong punctate echoes, and focal anechoic areas; (4) Vascular patterns were categorized as: eccentric hilar, or non-hilar (including mixed, peripheral, and avascular subtypes).

SWE method and image evaluation

The SL15-4 MHz transducer was gently positioned perpendicular to the neck skin surface with optimal acoustic coupling. A region of interest (ROI) was placed along the longitudinal axis of the LNs (LNs), encompassing the entire nodal parenchyma and adjacent soft tissues while avoiding calcifications and necrotic foci. Interfering factors, including the fluid area, pulsatile motion of major blood vessels, and bone structures [8], were present in the examined LNs. When the soft tissue around the LNs was uniformly blue or light green, images were captured and stored, with at least 3 2D-SWE sequences collected for each included. The system's preset superficial LNs mode utilized an elasticity color scale (0 – 100 kPa) with chromatic progression from blue (lowest stiffness) through green and yellow to red (highest stiffness). The 2D-SWE of subregional LNs is divided into [7-10]: (1) Uniformly blue coverage, where the entire LNs section is uniformly blue; (2) Blue-based mottled: the entire section is covered in a mosaic of colors, with blue comprising over 50% of the total area; (3) Non-blue-dominant heterogeneous coloration was defined as combined green-yellow-red spectrum distribution occupying >50% of the total sectional area. The Q-Box Trace method was utilized for tracing along the LNs (LNs) edge. Maximum strain wave envelope (Max -SWE, kPa) values were recorded across all 2D-SWE maps, and median values were calculated [9, 11].

CEUS method and image evaluation

An SL10-2MHz probe was employed, with a center frequency of 4.5 MHz and a mechanical index of 0.09. CEUS examination was performed by positioning the transducer along the longitudinal axis of the LNs. A 2.4 mL bolus of contrast agent (11.8 mg/mL) was administered intravenously via the antecubital vein, followed by a 5-mL saline flush, with continuous cine-loop acquisition maintained for 120 seconds after contrast mode activation CEUS enhancement patterns of LNs in this cohort were classified as follows based on established criteria [12]: (1) Uniform enhancement; (2) Heterogeneous enhancement, defined as the presence of perfusion defects or hypoperfused regions within LNs, with abnormalities classified as 'minor' (maximum hypoperfused area <50% of nodal cross-section) or 'major' (≥50%).

Statistical methods

SPSS 21.0 (IBM, USA) was utilized for statistical analysis. The count data of conventional US, SWE, and CEUS were analyzed using the $\chi 2$ test. The Max-SWE value was determined using the Wilcoxon rank-sum test. The AUC of the receiver operating characteristic curve was utilized to establish the Max-SWE threshold value for distinguishing between the two lesion groups. The sensitivity, specificity, accuracy, and area under the curve (AUC) of CEUS, 2D-SWE, and Max-SWE in the identification of LNs in the two groups were evaluated for differences. The statistical analysis was set at $\alpha = 0.05$, and statistically significant differences were observed between the groups.

RESULTS

Pathological result

Tuberculosis group: 35 cases (42 LNs). Metastasis group: 49 cases (49 LNs), including 14 cases of lung

[DOI: 10.61186/ijrr.24.1.8]

cancer (8 cases of adenocarcinoma, 3 cases of squamous cell carcinoma, 3 cases of small cell carcinoma), 10 cases of papillary thyroid carcinoma, 8 cases of metastatic poorly differentiated carcinoma, and laryngeal carcinoma. There were 3 cases of breast cancer, 3 cases of esophageal cancer, 2 cases of nasopharyngeal cancer, 1 case of bladder cancer, kidney cancer, cervical cancer, ovarian cancer, malignant melanoma and Kaposi's sarcoma.

Ultrasound results

General US features

As can be shown in table 1, there were no statistically significant differences in the involved area and anatomical location of cervical LNs between the TB group and the metastatic group (P>0.05). However, significant differences were observed in the short and long diameters of the included LNs (P<0.05). Table 2 demonstrates comparable Lhand S values, portal medulla morphology, internal echogenicity, and vascular patterns between the two groups (all P>0.05).

SWE and CEUS features

To examine the findings from table 3, it is evident that none of the LNs (LNs) in the 2D-SWE exhibited uniformly blue color. Within the tuberculosis (TB) group, 71.4% of the cases (30/42) displayed a predominantly blue appearance, while 69.1% of the cases (29/49) exhibited large-scale filling defect areas. Among these, 55.2% of the cases (16/29) showed "circular" enhancement, as demonstrated in Figure 1. In the transfer group, 57.1% (28amp 42) showed non-blue variegated color, and 75.5% (37max 42) saw small filling defect areas, as shown in figure 2.

Table 1. Anatomical location of enlarged cervical LNs and size of included LNs.

Group	Affected neck area [(%)]		Include LNs anatomical locations [(%)]					Size [($\bar{X}$±S)cm]	
	unilateral	bilateral	I region	II region	III region	IV region	V region	Short diameter	Long diameter
Tuberculosis [42]	24(57.1)	18(42.9)	1(2.4)	7(16.7)	5(11.9)	16(38.1)	13(30.9)	1.1±0.3	2.0±0.7
transfer [49]	23(46.9)	26(53.1)	0(0.0)	9(18.3)	14(28.6)	14(28.6)	12(24.5)	1.3±0.5	2.3±0.7
Statistics	χ2 value=0.943		χ2 value=3.980					Z value =-2.007	Z value =-2.085
***P* value**	0.332		0.264					0.045	0.037

Note: lymph node (LNs).

Table 2. Conventional US sonographic features of cervical LNs tuberculosis and metastatic LNs [number (%)].

Group	L/S		Lymphoid medulla morphology		internal echo		Blood flow type	
	≥2	<2	exist	disappear	uniform	uneven	Eccentric portal flow	Non-portal blood flow
Tuberculosis [42]	16(38.10)	26(61.90)	9(21.43)	33(78.57)	10(23.81)	32(76.19)	8(19.05)	34(80.95)
transfer [49]	15(30.61)	34(69.39)	4(8.16)	45(91.84)	6(12.24)	43(87.76)	3(6.12)	46(93.88)
χ2value/ *P* value	0.564/0.453		3.250/0.071		2.087/0.149		3.555/0.059	

Table 3. SWE and CEUS characteristics of cervical LNs tuberculosis and metastatic LNs [(%)].

	2D-SWE			CEUS		
	uniform blue	Blue-based variegation	Non-blue-based variegated colors	Uniform enhancement	Non-uniform enhancement	
					Small-scale abnormal perfusion	Extensive abnormal perfusion
tuberculosis (42)	0(0.0)	30(71.4)	12(28.6)	4(9.5)	9(21.4)	29(69.1)
transfer (49)	0(0.0)	21(42.9)	28(57.1)	3(6.1)	37(75.5)	9(18.3)

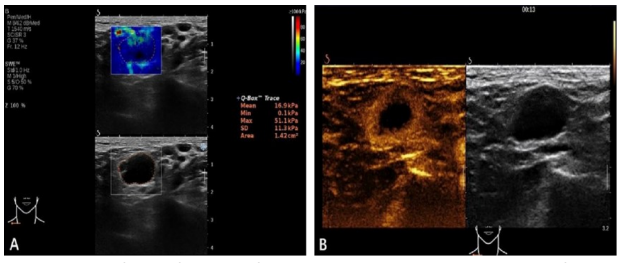

Figure 1. Tuberculosis with caseous necrosis **A:** 2D-SWE shows "blue-dominated variegation", with a black "dark area" without color filling in the center, Max-SWE=51.1 kPa; **B:** A large area of non-perfusion is seen in the CEUS node, showing "ring" enhancement.

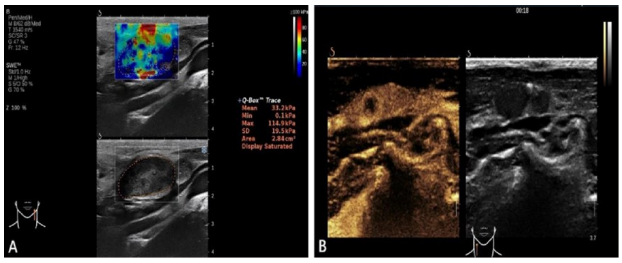

Figure 2. Lung adenocarcinoma **A:** 2D-SWE is "non-blue-based variegated colors", that is, green, yellow, and red colors are the main colors, Max-SWE=114.90kPa; **B:** Small area without perfusion in CEUS nodules.

The texture characteristics of the tuberculosis group exhibited a slightly soft texture, with a Max-SWE value of 63.4±23.5 kPa (35.9 kPa~121.0 kPa). In contrast, the metastatic group displayed a harder texture, with a Max-SWE of 104.2±58.6 kPa (45.6 kPa~300.0 kPa). The differences between the two groups were statistically significant. Significant (Z value=-3.097, P=0.002), using the ROC curve, the Max-SWE cutoff value of the two groups was determined to be 76.3 kPa, that is, the tuberculosis group was <76.3 kPa, and the metastasis group was ≥76.3 kPa. In addition, there are 23 LNs with Max-SWE>100kPa in this data, including 5 tuberculosis (figure 3A), 18 metastatic (5 lung or nasopharyngeal squamous cell carcinoma, 3 lung adenocarcinoma, 2 small cell carcinomas, 2 papillary thyroid carcinomas, 2

[DOI: 10.61186/ijrr.24.1.8]

metastatic poorly differentiated carcinomas, 1 invasive ductal carcinoma of the breast, 1 ovarian cancer, 1 malignant melanoma, and 1 Kaposi's sarcoma, figure 3B).

Comparison of diagnostic performance between SWE and CEUS

As shown in table 4, if metastatic LNs (LNs) are diagnosed using '2D-SWE showing non-blue color,' 'Max-SWE≥76.3 kPa,' or 'small abnormal perfusion or uniform enhancement in CEUS node,' the diagnostic efficiency of CEUS is moderate (AUC=0.753), while that of 2D-SWE and Max-SWE is lower (AUC=0.643 and 0.605, respectively). CEUS has the highest sensitivity (Se=81.6%) and specificity (A=75.8%), while 2D-SWE has the highest specificity (Sp=71.4%).

Table 4. Differentiation of cervical LNs tuberculosis and metastatic LNs by SWE and CEUS [number (%)].

	2D-SWE		Max-SWE		CEUS	
	Blue-based variegation	Non-blue-based variegated colors	<76.3 kPa	≥76.3 kPa	Large-scale abnormal perfusion	Small area abnormal perfusion/ uniform enhancement
tuberculosis [42]	30(71.4)	12(28.6)	26(61.9)	16(38.1)	29(69.1)	13(30.9)
transfer [49]	21(42.9)	28(57.1)	20(40.8)	29(59.2)	9(18.4)	40(81.6)
χ2value/ *P*v alue	7.494/ 0.006		4.024/ 0.045		42.496/ 0.000	
Se/ Sp/ A	57.1%/ 71.4%/ 63.7%		59.2%/ 61.9%/ 60.4%		81.6%/ 69.1%/ 75.8%	
AUC (95% CI)	0.643 (0.529,0.757)		0.605 (0.489,0.722)		0.753 (0.650,0.857)	

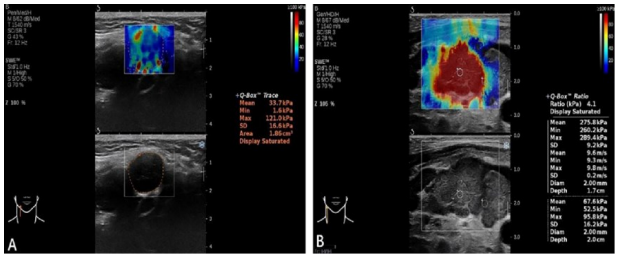

Figure 3. A: Tuberculosis, Max-SWE=121.00kPa; **B:** Nasopharyngeal squamous cell carcinoma, Max-SWE=289.40kPa.

DISCUSSION

A meta-analysis demonstrated that elastography exhibited a sensitivity of 81% (95% CI: 72-88%) in distinguishing benign from malignant LNs, with a specificity of 85% (95% CI: 70-93%). Differences in the types of pathology included serve as a significant reason for the observed heterogeneity among these studies [13], with most studies including no or only a limited number of cases of tuberculosis. CEUS has demonstrated strong diagnostic efficacy for evaluating LNs traditionally challenging to identify via conventional ultrasound [11, 12]. However, the use of CEUS is limited due to the adaptation of SonoVue into the population, economic burden, and allergic risk. Subsequently, this study aims to evaluate the diagnostic value of the two methods in differentiating between metastatic LNs and tuberculosis, serving as a guide for ultrasound specialists to select the most appropriate technique.

SWE is a novel elastic ultrasound technology that not only displays two-dimensional elastograms, akin to strain elastography (SE), but also quantitatively assesses tissue stiffness. SE employed color maps to visualize the elastic differences between LNs and further established diagnostic criteria based on the proportion of hard areas within each LNs cross-section relative to the total cross-sectional area. The number of classifications across various criteria spanned a range of 4 to 8 [7, 8, 10, 12]. As SE increasingly transitions to SWE (SWE), the cumbersome diagnostic standards previously reliant on SE have largely been abandoned. However, color elastography is intuitive, simple, and has good clinical usability. Bhatia *et al.* [14] proposed that the 2D-SWE of LNs can be categorized into uniform blue and non-uniform blue, with the latter not further subdivided due to the limited number of cases. Following the aforementioned research and considering the characteristics of this dataset group, a simplified 2D-SWE standard has been proposed, comprising three categories: uniformly blue, blue-based variegated color, and non-blue-based variegated color. This standard aims to detail the hardness differences between LNs. In addition, in this study, the Max-SWE value was measured after tracing the maximum section of the LNs using the trajectory method. Additionally, many studies considered the Max value to be the most suitable quantitative index for reflecting LNs lesions [9], and it was also an independent predictor of malignant LNs.

In this dataset, the hardness of the metastatic group is high, while that of the tuberculosis group is low, which may be associated with pathological features and the course of the disease. In the metastatic group, the largest LNs had a Max-SWE value of 300.0 kPa, and 18 LNs exhibited SWE values above 100 kPa, with only 3 of these 18 LNs exhibiting punctate calcification. It is evident that calcification is not the primary cause for the increase in LNs hardness. Instead, it may be due to rapid tumor cell proliferation within nodal tumor cells over a short period, resulting in an increase in intranodal pressure. LNs hardness in squamous cell carcinoma metastasis has been reported to be very high. This group of Max value > 100 kPa squamous cell carcinoma accounted for 71.4 % of all squamous cell carcinoma (5/7) [15]. When an abscess forms in the LNs, a colorless, fully black 'dark area' (as shown in Figure 1-A) may appear, appearing black because shear waves cannot propagate in the fluid, making it appear black. When certain pathological changes, including granulomas, caseous necrosis, fibrous tissue

[DOI: 10.61186/ijrr.24.1.8]

hyperplasia, and coarse calcification, occur in the LNs, the stiffness of the LNs increases. However, unlike metastatic LNs, which are caused by a large number of proliferating tumor cells, only 5 instances of tuberculosis-associated LNs with a Max-SWE value greater than 100.0 kPa were observed, with a maximum value of 121.0 kPa.

The primary advantage of CEUS is that it can clearly demonstrate areas of no enhancement or low enhancement within the LNs [11]. Among the LNs (e.g., 83/91) in this group, approximately 92.3% exhibited evidence of abnormal perfusion characteristics. LNs with tuberculous involvement and metastatic LNs necrosis are commonly observed in pathological sections, including: (1) clastic necrosis (the early stage of coagulation-induced necrosis caused by various pathological etiologies), which is commonly seen in metastatic tumors and tuberculous cases; (2) Caseous necrosis is most common in tuberculosis; (3) Purulent necrosis, that may be secondary to caseous necrosis of TB, is often accompanied by the development of purulent liquefaction [16]. It is evident that clastic and coagulative necrosis commonly occur in metastatic LNs. Small areas of necrosis are challenging to visualize using conventional US imaging, though they can be clearly identified using CEUS. Caseous necrosis and suppurative necrosis are more commonly associated with cases of tuberculosis. Despite the wide range, gray-scale US images frequently exhibit hypoechoic regions, which can make it challenging to differentiate them from LNs. However, CEUS clearly demonstrates that typical cases of tuberculosis exhibit "circular enhancement" [12].

A limitation of this study is that the loss of medullary structures in most included LNs prevents the identification of some early-stage metastatic LNs and tuberculous LNs. At present, the recognition of this type of LNs remains a significant challenge in ultrasound imaging, which requires further investigation in the future.

In summary, SWE should be the first choice in cases where conventional US is indicative of metastatic LNs or tuberculosis. A significant proportion of metastatic LNs exhibited high levels of hardness, whereas most nodules showed low levels of hardness. SWE exhibited a specificity of 71.4%, however, its accuracy was marginally lower at 63.7%. When further identification is required, CEUS is feasible. Additionally, the black dark area of 2D-SWE or the no perfusion area of CEUS should be avoided during the procedure to improve the qualified rate of puncture biopsy.

***Acknowledgements*:** None.
***Funding*:** Not applicable.
***Availability of data and materials*:** The datasets used and/or analyzed during the current study are available from the corresponding author on reasonable request.
***Ethics approval and consent to participate*:** The study was approved by the hospital's ethics committee.
***Consent for publication*:** The patients have given their consent for publication. Written informed consent was obtained from the patients for publication of this Case report and any accompanying images. A copy of the written consent is available for review by the Editor of this journal.
***Competing interests*:** The authors declare that they have no competing interests.
Authors' Contributions: J.F., was a major contributor to writing the manuscript. F.S., collected the patient data. T.S., performed both surgeries and followed up the patients. X.W., realized the scarcity of the two cases, did literature searches, and revised the manuscript. All authors read and approved the final manuscript.

REFERENCES

1. Vaughn JA (2023) Imaging of pediatric cervical lymphadenopathy. *Neuroimaging Clin N Am, **33**(4): 581-590.*
2. Bran W, Sahli-Vivicorsi S, Cadieu R, Alavi Z, Leclere JC (2023) Ultrasound-guided hookwire localization of non-palpable cervical lymphadenopathy: A case-control study of operative time. *Cancer Med, **12**(15): 16054-16065.*
3. Majeed FA, Raheem K, Zafar U, Chatha SS, Raza A, Rauf A (2023) Cervical mediastinoscopy as a diagnostic tool for mediastinal lymphadenopathy. *J Coll Physicians Surg Pak, **33**(9): 1062-1066.*
4. Golemati S and Cokkinos DD (2022) Recent advances in vascular ultrasound imaging technology and their clinical implications. *Ultrasonics, **119**: 106599.*
5. Shen Y, He J, Liu M, Hu J, Wan Y, Zhang T, Ding J, Dong J, Fu X (2024) Diagnostic value of contrast-enhanced ultrasound and shear-wave elastography for small breast nodules. *PeerJ, **12**: e17677.*
6. He H, Wu X, Jiang M, Xu Z, Zhang X, Pan J, Fu X, Luo Y, Chen J (2023) Diagnostic accuracy of contrast-enhanced ultrasound synchronized with shear wave elastography in the differential diagnosis of benign and malignant breast lesions: a diagnostic test. *Gland Surg, **12**(1): 54-66.*
7. Lee HY, Lee JH, Shin JH, Kim SY, Shin HJ, Park JS, Choi YJ, Baek JH (2017) Shear wave elastography using ultrasound: effects of anisotropy and stretch stress on a tissue phantom and in vivo reactive lymph nodes in the neck. *Ultrasonography, **36**(1): 25-32.*
8. Acu L, Oktar S, Acu R, Yücel C, Cebeci S (2016) Value of ultrasound elastography in the differential diagnosis of cervical lymph nodes: A comparative study with b-mode and color doppler sonography. *J Ultrasound Med, **35**(11): 2491-2499.*
9. Lo WC, Hsu WL, Wang CT, Cheng PW, Liao LJ (2019) Incorporation of shear wave elastography into a prediction model in the assessment of cervical lymph nodes. *PLoS One, **14**(8): e0221062.*
10. Chiorean L, Barr RG, Braden B, Jenssen C, Cui XW, Hocke M, Schuler A, Dietrich CF (2016) Transcutaneous ultrasound: elastographic lymph node evaluation. current clinical applications and literature review. *Ultrasound Med Biol, **42**(1): 16-30.*
11. Tan S, Miao LY, Cui LG, Sun PF, Qian LX (2017) Value of shear wave elastography versus contrast-enhanced sonography for differentiating benign and malignant superficial lymphadenopathy unexplained by conventional sonography. *J Ultrasound Med, **36**(1): 189-199.*
12. Jung EM, Jung F, Stroszczynski C, Wiesinger I (2021) Quantification of dynamic contrast-enhanced ultrasound (CEUS) in non-cystic breast lesions using external perfusion software. *Sci Rep, **11**(1): 17677.*
13. Kang HJ, Seo M, Sohn YM, Yun SJ, Min SY, You MW, Yeon EK (2019) Comparison of diagnostic performance of b-mode ultrasonography and shear wave elastography in cervical lymph nodes. *Ultrasound quarterly, **35**(3): 290-296.*
14. Bhatia KS, Cho CC, Tong CS, Yuen EH, Ahuja AT (2012) Shear wave

[DOI: 10.61186/ijrr.24.1.8]

elasticity imaging of cervical lymph nodes. *Ultrasound Med Biol,* ***38*** *(2): 195-201*.

15. Azizi G, Keller JM, Mayo ML, Piper K, Puett D, Earp KM, Malchoff CD (2016) Shear wave elastography and cervical lymph nodes: predicting malignancy. *Ultrasound Med Biol,* ***42****(6): 1273-1281*.
16. Martinez-Cabriales SA, Walsh S, Sade S, Shear NH (2020) Lymphomatoid papulosis: an update and review. *Journal of the European Academy of Dermatology and Venereology: JEADV,* ***34*** *(1): 59-73*.

[DOI: 10.61186/ijrr.24.1.8]